1 **Rapid evolutionary change in trait correlations of a single protein**
2
3
4 Pouria Dasmeh[1,3*], Jia Zheng[5*], and Andreas Wagner[1,2,3,4]

5 [1]Institute for Evolutionary Biology and Environmental Studies, University of Zurich, Zurich,
6 Switzerland. [2]The Santa Fe Institute, Santa Fe, New Mexico, [3]Swiss Institute of Bioinformatics
7 (SIB). [4]Stellenbosch Institute for Advanced Study (STIAS), Wallenberg Research Centre at
8 Stellenbosch University, Stellenbosch 7600, South Africa. [5]Westlake Institute for Advanced
9 Study, Hangzhou, China. (*Equal contribution)

10

11 **Abstract:**

12 Many organismal traits are genetically determined and covary in evolving populations.

13 The resulting trait correlations can either help or hinder evolvability – the ability to bring

14 forth new and adaptive phenotypes. The evolution of evolvability requires that trait

15 correlations themselves must be able to evolve, but we know little about this ability. To

16 learn more about it, we here study one of the simplest evolvable systems, a gene

17 encoding a single protein, and two traits of this protein, namely the ability to emit yellow

18 and green light. We show that correlations between these two traits can evolve rapidly

19 through both mutation and selection on short evolutionary time scales. In addition, we

20 show that these correlations are driven by a protein's ability to fold, because single

21 mutations that alter foldability can dramatically change trait correlations. Since foldability

22 is important for most proteins and their traits, mutations affecting protein folding may

23 alter trait correlations mediated by many other proteins. Thus, mutations that affect

24 protein foldability may also help shape the correlations of complex traits that are

25 affected by hundreds of proteins.

26
27

28

29

30

31

32   **Body:**

33   Evolvability is a biological system's ability to bring forth novel and adaptive phenotypes.

34   Because evolvability varies among organisms and traits, it can itself evolve[1].

35   Understanding the factors that affect its evolution matters not only for our fundamental

36   understanding of biological evolution. It also matters for technological applications,

37   including the experimental evolution of novel and useful molecules such as efficient

38   industrial enzymes[2].

39   Many phenotypic traits are correlated with one another, and these correlations

40   often have a genetic basis[3-5] . Examples of such traits include the weight and the height

41   of individuals within a population[6]. They also include coloration and behavioral traits in

42   many animal species [3,7,8], as well as seed dormancy and flower time in plants [9]. Genetic

43   correlations between phenotypic traits can influence evolvability, because they can

44   affect the extent to which traits can evolve independently from one another[10-14].

45   On the one hand, correlated trait evolution can facilitate evolvability. For

46   example, in species of freshwater fish from the genus *Micropterus*, a strong correlation

47   between mouth and jaw morphology helps these species adapt to the consumption of

48   large prey [15,16]. On the other hand, strong trait correlations can also hamper evolvability,

49   rendering weak trait correlations advantageous. For example, a weak correlation

50   between early tetrapod forelimb and hindlimb morphology helped bring forth major

51   specializations, such as bipedalism and flight[17,18]. More generally, the decoupling of

52   traits from one another helps trait variation become individuated within a population,

53   such that genetic change can affect only one trait without affecting others. Trait

54   individuation can help explain phenomena as different as the evolution of different cell

55 types in multicellular organisms[19], leaf shapes in plants[20], and body structures in

56 animals[21].

57   Because trait correlations are important for evolvability, it is important to study

58 how easily these correlations can themselves evolve. Previous studies have shown that

59 trait correlations can change on evolutionary time scales, and become weaker or

60 stronger in some lineages of different species. For example, the correlation between

61 beak and the skull morphology in Darwin's Galapagos finches (genus *Geospiza*) and

62 Hawaiian honeycreepers (*Drepanis coccinea*) is significantly stronger compared to their

63 continental relatives[22], which has facilitated rapid craniofacial evolution in the former

64 species. Another example is indigenous Australian *dicotyledon* species where the

65 correlations between several seedling traits such as the patterns of scale-like leaves are

66 evolutionarily malleable across thousands of species[23]. Although examples like these

67 show that trait correlations can evolve, we know little about how rapidly they can do so.

68 In addition, we cannot easily quantify the contribution of mutations and selection to

69 these correlations and their evolutionary change. The reason is that they are complex

70 traits of multicellular organisms, which may be influenced by dozens or hundreds of

71 genes. Also, it is difficult to determine the causes of correlations between complex traits.

72 In principle, they can be caused by genetic factors, such as pleiotropy and linkage

73 disequilibrium [24], and by environmental and ecological factors, such as habitat

74 temperature and aridity [25,26].

75   To overcome some of these challenges, we study evolutionary change in trait

76 correlations for one of the simplest possible evolving systems, namely a single protein-

77 coding gene. If trait correlations can easily evolve in this simple study system, they

78 would probably be even more malleable in the sets of interacting genes that determine

79 complex macroscopic traits. Our focal gene of interest is *yfp*, which encodes yellow

80 fluorescent protein (YFP). Because this protein plays no important biological role in the

81 microbial host organism *E. coli* in which we study it, we can examine its traits

82 independently from complicating interactions with the genetic background in which it

83 occurs. YFP emits both yellow and green fluorescence light, and these emissions are

84 the two traits we study (Figure 1A). They can be quantified rapidly and precisely in

85 thousands of organisms through fluorescence activated cell sorting (FACS), which also

86 allows us to precisely estimate trait correlations.

87   Single point mutations can shift the maximum emission wavelength of YFP. This

88 property facilitates the experimental evolution of fluorescence color in YFP-expressing

89 cell populations. In addition, it allows us to ask whether mutation and/or selection can

90 change the correlation between yellow and green fluorescence. To do so, we

91 systematically measure this correlation in both genetically polymorphic populations of

92 *E.coli* cells that express different YFP variants, as well as in isogenic populations of

93 several YFP mutants. In addition, we also measure this correlation in YFP

94 subpopulations that differ in their fluorescence intensities. These experiments enable us

95 to distinguish the extent to which microenvironmental variation (gene expression noise),

96 mutation, and selection affect the correlation between two traits of a single protein.

97   Before starting our main experiments, we needed to exclude the contribution of

98 two confounding factors. First, even cells that do not express fluorescent proteins often

99 exhibit some background-fluorescence resulting from other fluorescing molecules [27]. To

100 exclude the possibility that such autofluorescence may explain the trait correlations we

101   might observe for YFP, we first measured both the yellow and green autofluorescence

102   of *E.coli* cells that do not express YFP. To this end, we used multicolor flow cytometry

103   with two spatially separated lasers, and recorded fluorescence intensity in the yellow

104   and green channels of the cytometer (Methods). The two autofluorescence traits are

105   only weakly correlated (Spearman's rank correlation R=0.03, p=0.0002;) (Figure 1B).

106   Any significantly stronger correlations in YFP-expressing cells can be attributed to YFP,

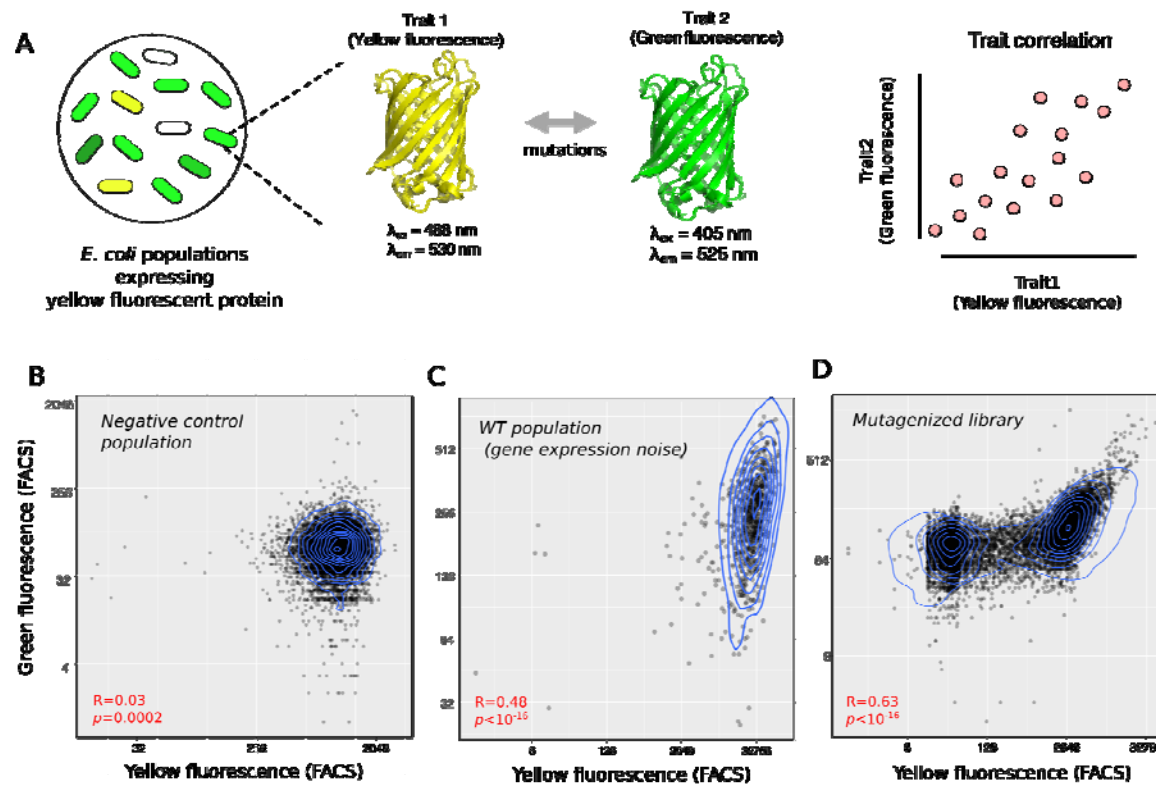107   and not to cellular autofluorescence.

108

109

110

111

112

113

114
115
116 **Figure 1. Gene expression noise and mutations can change the strength of correlation**
117 **between yellow and green fluorescence intensities.** A) Schematic of experimental design.
118 We investigate the correlation between yellow and green fluorescence intensities in E. coli
119 populations that express yellow fluorescent protein (YFP). B) Autofluorescence correlation
120 between yellow and green fluorescence intensities in an *E.coli* population without the *yfp* gene.
121 C) The correlation between yellow and green fluorescence intensities in an isogenic population
122 expressing wild-type YFP protein. D) The correlation between yellow and green fluorescence
123 intensities in a mutagenized YFP library, where each YFP molecule has, on average, ~ 1 amino
124 acid mutation. Data in panels B-D are based on fluorescence-activated cell sorting (FACS) with
125 ~10^5 sorted cells (see Methods for details). Blue lines in panels B-D show the contours of a two-
126 dimensional density of data points.
127
128

6

129   A second confounding factor is a correlation in fluorescence that is not caused by

130   YFP itself but by the environment. Although the external environment (medium and

131   temperature) of our *E.coli* cells did not change during our experiments (see Methods),

132   the microenvironment inside a cell can also affect phenotypic traits. For example, this

133   environment fluctuates constantly due to the thermal molecular motions of its

134   molecules, which causes noisy expression of all genes[28,29]. To identify trait correlations

135   caused by such environmental variation, we measured the correlation between yellow

136   and green fluorescence intensities in a population of isogenic (genetically identical)

137   *E.coli* cells that express wild-type YFP (Figure 1C). Because all cells in such a

138   population have the same genotype, only (micro)environmental variation can contribute

139   to any observed trait correlation in the population. We observed a significant correlation

140   between the two traits (Spearman's rank correlation R=0.48, $p < 10^{-16}$) that was 16

141   times higher than in autofluorescing cells (R=0.03, $p < 10^{-16}$, Spearman's rank

142   correlation; Figure 1C). This correlation is not unexpected and can be explained by

143   gene expression noise. The reason is that the fluorescence intensity of a single cell is

144   proportional to the abundance of its YFP molecules. Cells with highly expressed YFP

145   will thus fluoresce more intensely in both green and yellow, compared to cells with lowly

146   expressed YFPs, which leads to the substantial environmental trait correlation we

147   observed.

148   We next turned to one of our central questions, namely whether mutations can

149   strengthen or weaken this baseline correlation. To find out, we measured yellow and

150   green fluorescence in a library of YFP proteins that we had created by error-prone PCR

151   mutagenesis [30,31]. YFP variants in this library had on average one single point mutation.

152 In this library, we observed a correlation between the two fluorescence intensities

153 (R=0.63, $p < 10^{-16}$, Spearman's rank correlation; Figure 1D), that was significantly

154 stronger than the correlation caused only by gene expression noise ($p \sim 0$, Fisher's z-

155 transformation). This shows that mutations can readily alter the correlation between our

156 focal traits. We explore the reasons further below.

157   To investigate whether selection can affect trait correlations as well, we

158 measured the correlation between yellow and green fluorescence intensities in three

159 YFP populations that we had previously evolved under multiple cycles of mutation and

160 either strong selection, weak selection, or no selection for yellow fluorescence intensity

161 [30,31] (Figure 2A, see Methods for details). The properties of the YFP protein variants in

162 these populations differ from that of wild-type YFP. For example, the ratio of the median

163 yellow fluorescence intensity of YFPs in populations that evolved under no selection,

164 and either weak or strong selection to that of an isogenic YFP wild-type (WT) population

165 was $\sim$ 0.68, $\sim$ 1, $\sim$18, respectively. Previous single-molecule real-time sequencing had

166 also shown that during this experimental evolution, YFP accumulated up to ~6 amino

167 acid changes compared to the wild-type [30].

168   Indeed, trait correlation increased from R=0.5 ($p < 10^{-16}$, Spearman's rank

169 correlation) for the YFP populations that had evolved under no selection, to R=0.78 and

170 R=0.82 ($p < 10^{-16}$, Spearman's rank correlation), for the populations that had evolved

171 under weak and strong selection, respectively (Figure S1). Because we suspected that

172 trait correlations may depend on absolute fluorescence intensities, we pooled YFPs

173 from these three populations and further partitioned this pooled population into 20

174 subpopulations, such that each subpopulation spanned a similar interval of yellow

175   fluorescence intensity (see Methods). We then sorted ~10^5 cells in each subpopulation

176   using fluorescence-activated cell sorting (Figures 2B), and measured the correlation

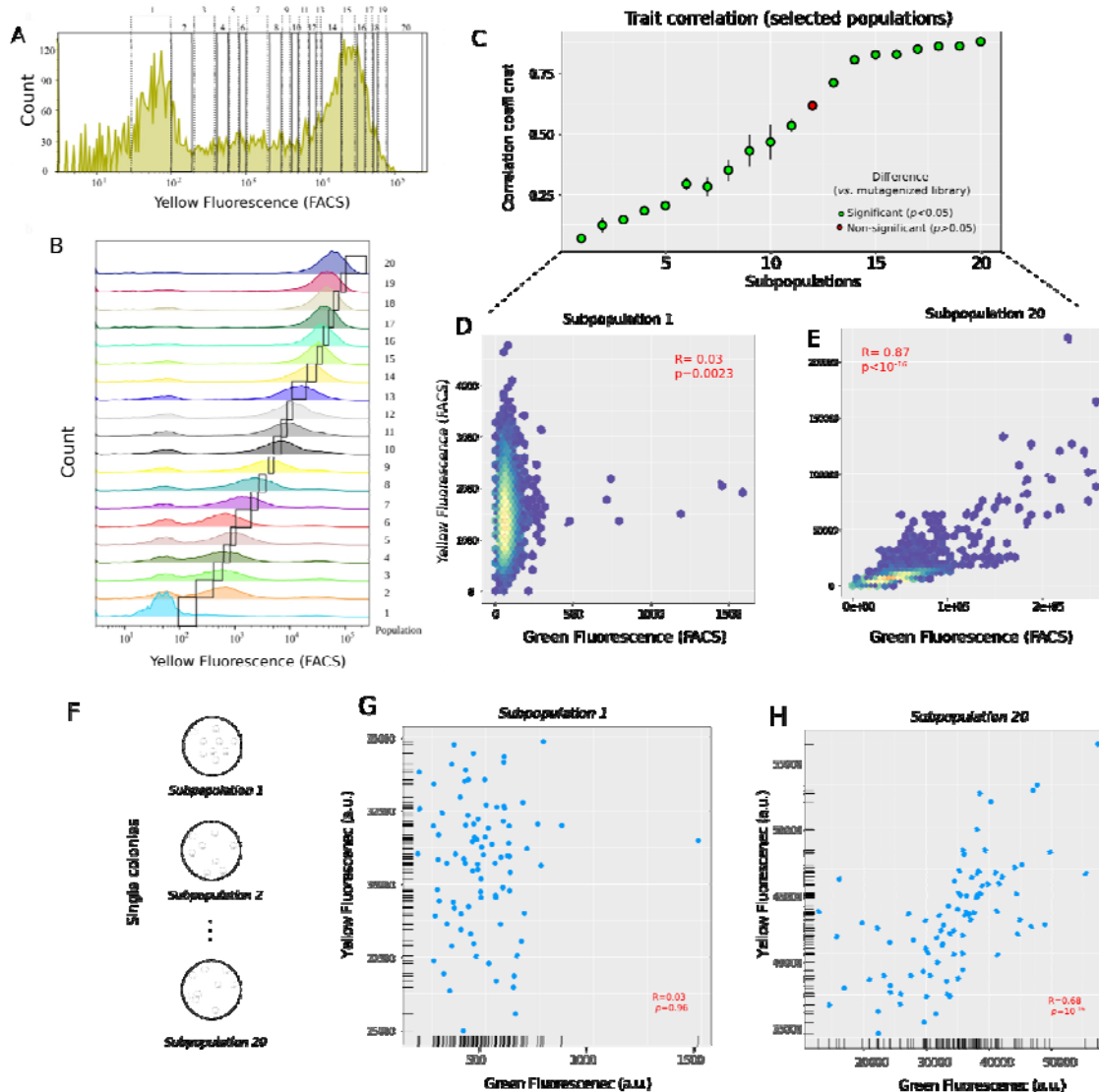177   between yellow and green fluorescence intensities in each subpopulation.

178

Figure 2

179

180   **Figure 2. Selection systematically changes the trait correlation measured at the level of**
181   **single cells.** A) Distribution of fluorescence intensity from fluorescence-activated cell sorting (FACS) of
182   our pooled population, which contains YFP variants that have evolved under mutation and various

9

183   strengths of selection to maintain yellow fluorescence (Methods), and that display different fluorescence

184   intensities. The vertical axis indicates the number of cells at a given yellow fluorescence intensity

185   (horizontal axis, arbitrary units). To study cells of different fluorescence intensity, we sorted cells from this

186   population into twenty bins (subpopulations) according to this yellow fluorescence intensity

187   (Subpopulations 1 to 20, as indicated by lettering on top of each bin). B) Each of the subpanels from

188   bottom to top shows the distribution of fluorescence intensities of cells in one of the 20 subpopulations

189   (right vertical axis). C) Spearman's correlation coefficient for the correlation between yellow and green

190   fluorescence intensities in all 20 subpopulations (indicated on the x-axis). Error bars represent the

191   standard deviation of the correlation coefficient, as measured from three replicate samples of the same

192   subpopulation. Green circles correspond to subpopulations in which the correlation between yellow and

193   green fluorescence was significantly different from that caused by single point mutations ($p < 0.05$). The

194   red circle corresponds to the 12th subpopulation, in which this correlation was statistically

195   indistinguishable from that caused by mutation ($p < 0.05$). We compared the significance of the trait

196   correlation in each subpopulation with the correlation caused by mutations (R=0.63, p $< 10^{-16}$,

197   Spearman's rank correlation), using Fisher's z-transformation (see Methods). D) Yellow fluorescence

198   intensity versus green fluorescence intensity for the first subpopulation (with lowest fluorescence

199   intensity). E) Yellow fluorescence intensity versus green fluorescence intensity for the 20th subpopulation

200   (with the highest fluorescence intensity). F) We picked 90 single clones from each of our twenty

201   subpopulations, and measured the correlation between yellow and green fluorescence intensities in liquid

202   cultures derived from each of these 1800 (=90x20) colonies (see Methods). Yellow fluorescence intensity

203   versus green fluorescence intensity for the 90 clones sampled from G) the first subpopulation and H) the

204   20th subpopulation. All correlation coefficients (R) are Spearman's rank correlations.

205

206   Remarkably, the correlation between yellow and green fluorescence varied

207   dramatically among the 20 subpopulations. It increased from a weak correlation

208   (R=0.03, $p = 0.00023$; Spearman's rank correlation) for the first subpopulation with the

209   lowest average yellow fluorescence intensity, to a strong correlation (R=0.87, $p < 10^{-16}$;

210   Spearman's rank correlation) for the 20th subpopulation with the highest average yellow

211   fluorescence intensity (Figures 2C-E). The correlation between yellow and green

212   fluorescence was significantly different ($p < 0.05$; Fisher's z-transformation, Methods)

213   from that caused by mutations (Spearman's R=0.63) for all except the 12th

214   subpopulation ($p \sim 0.3$, Fisher Z-transformation). These results show that selection can

10

215   systematically change the strength of a trait correlation, and render it significantly

216   stronger or weaker than the one caused by mutations. To further validate this

217   observation, we picked 90 single clones from each of the 20 subpopulations and

218   measured their yellow (λ_{ex} = 485 nm, λ_{em} = 530 nm) and green (λ_{ex} = 400 nm, λ_{em} = 512

219   nm) fluorescence intensities using a microplate reader (TECAN Spark) (Figure 2F, see

220   Methods for details). For these single clones too, we observed an increase in the

221   correlation of the green and yellow fluorescence intensities from the first subpopulation

222   to the 20th subpopulation (Figure 2G-H). Altogether, our observations show that trait

223   correlations can be easily shaped by selection, even on the short time scales of

224   laboratory evolution.

225   We next focused on trait correlations in individual YFP mutants that had

226   appeared in our evolving populations during experimental evolution. We reasoned that

227   these variants might help us find out why trait correlations can vary so strongly from one

228   subpopulation to another. Specifically, we measured trait correlations for 71 YFP

229   mutants that we had previously engineered, because they attained moderate to high

230   frequency in evolving populations [30,31]. These variants include the WT protein, as well

231   as 10 mutants with one, 28 mutants with two, and 32 mutants with three amino acid

232   changes (Table S1). All double mutations share the mutation G66S (replacement of a

233   glycine with serine at position 66 of YFP) or Y204C, and all triple mutations share both

234   amino acid changes G66S and Y204C. The mutations G66S and Y204C are unique in

235   that they shift the emission spectrum of YFP from yellow towards green fluorescence[30].

236   Trait correlations varied significantly among isogenic populations expressing

237   these mutants (Figure 3A). Specifically, they varied from R=0.17 (for the triple mutant

238   G66S-Y204C-F72S; $p < 10^{-16}$, Spearman's rank correlation) to R=0.98 (for the double

239   mutant G66S-N145S, $p < 10^{-16}$; Spearman's rank correlation). Remarkably, some single

240   point mutations sufficed to substantially strengthen (Figure 3B) or weaken (Figure 3C)

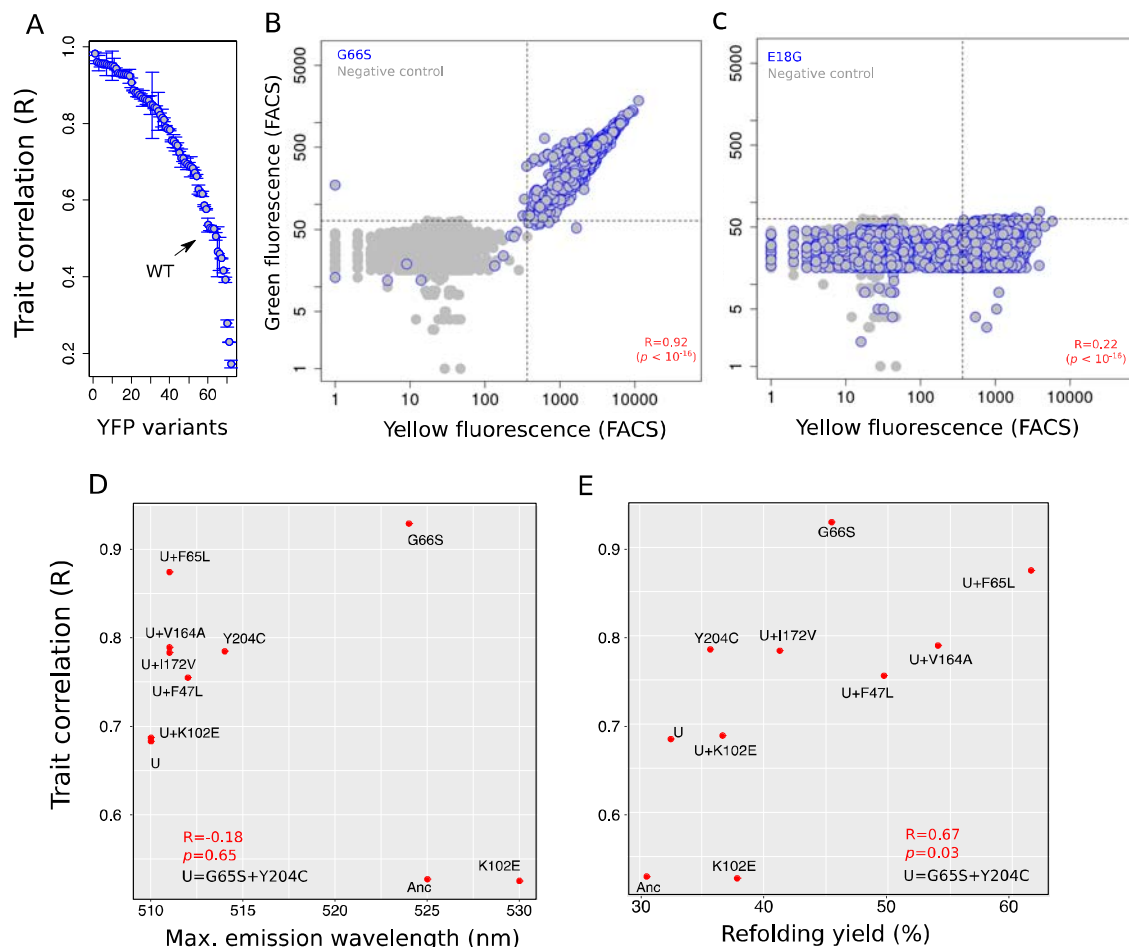241   the trait correlation of the WT protein.

242

Figure 3

243

244   **Figure 3. Trait correlation substantially changes by single point mutations that affect protein**
245   **folding.** A) The correlation between yellow and green fluorescence intensities varies substantially in
246   isogenic populations of YFP variants. Each circle corresponds to data from a YFP variant, and error bars
247   show one standard deviation of Spearman's rank correlation coefficient between yellow and green
248   fluorescence intensities in three biological replicates of isogenic populations expressing the variant.

249   Green fluorescence intensity versus yellow fluorescence intensity for an isogenic population of B) the
250   mutant G66S, and C) the mutant E18G. For both panels B and C, gray circles represent cells from a
251   negative control population that does not express *yfp*. Blue circles represent cells from an isogenic
252   population of the respective mutant. Spearman's rank correlation coefficient between yellow and green
253   fluorescence intensities versus D) maximum emission wavelength (nm) for a selected set of 10 mutants,
254   and E) refolding yield after thermal denaturation for the same mutants. In panels D-E, the symbol U
255   represents the genotype G66S-Y204C. All correlation coefficients are Spearman's rank correlations.

256

257   We next asked which YFP properties can (i) be easily shaped by one or few mutations,

258   and (ii) affect the trait correlations we observe in individual variants and in our

259   polymorphic subpopulations. One candidate property is fluorescence color itself.

260   Mutations in YFP, particularly those that alter amino acids close to the protein's

261   fluorophore, can shift the emission spectrum of the protein. We compared trait

262   correlations for a set of 10 YFP variants that maximally emit in colors ranging between

263   yellow (~525-530 nm) and green (~510 nm; see Table S2). However, a change in this

264   emission maximum was not significantly associated with an altered trait correlation

265   (R=0.28, *p*=0.42; Spearman's rank correlation). For example, although the maximum

266   emission wavelength was substantially different between the mutant G55S (~ 521 nm)

267   and the triple mutants Y204C-G66S-F65L (~ 511 nm), the trait correlation is nearly the

268   same in these two mutants (~ 0.9). Another example involves the triple point mutants

269   that contain both color-shifting mutations Y204C and G66S (~ 511 nm). Among all such

270   mutants, trait correlation varied from 0.68 (for Y204C-G66S-K102E) to 0.87 (Y204C-

271   G66S-F65L). These observations show that the fluorescence color itself. i.e., the

272   emission spectrum, is not the key property affecting the trait correlations we study.

273   We then focused on a second candidate property, which is biophysical in nature.

274   It is the ability of a protein to fold properly. We hypothesized that changes in protein

13

275   foldability can affect trait correlations, because only folded proteins fluoresce. To

276   validate this hypothesis, we estimated the foldability of our 10 YFPs variants.

277   Specifically, we measured the overall refolding yield of YFP upon thermal denaturation

278   (see Methods). In this assay, we first denatured YFP, allowed it to refold, and quantified

279   the amount of re-folded proteins by measuring the fluorescence relative to the

280   fluorescence of YFPs that had not denatured[30]. Importantly, more foldable YFP variants

281   showed a significantly higher correlation between green and yellow fluorescence

282   intensities (Figure 3E; R=0.67, *p*=0.03; Spearman's rank correlation). Some of our 10

283   YFP variants in this analysis harbored the known foldability-improving mutations F47L,

284   V164A, and F65L[30]. The presence of these mutations alone increased the trait

285   correlation. For example, the trait correlation of the variant G65S-Y20C increased from

286   ~ 0.61 to ~ 0.75, 0.78, and 0.87, in the presence of the mutation F47L, V164A and
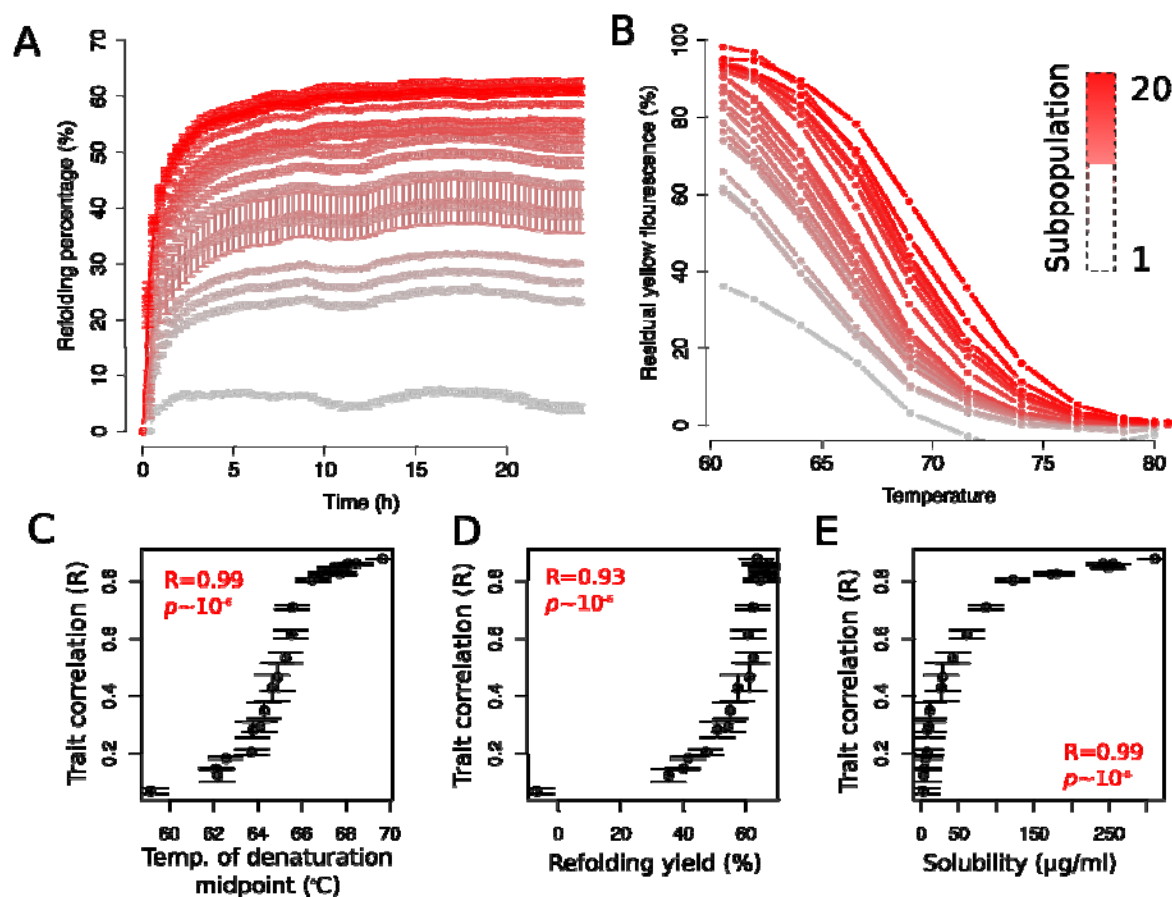
287   F65L, respectively (Table S2).

14

Figure 4. Foldability and solubility of YFP drive trait correlations in YFP populations. A) Refolding percentage upon thermal denaturation for the 20 subpopulations versus time (in hours). B) Residual yellow fluorescence as a function of temperature, for the 20 subpopulations. In panels A and B, subpopulations are color coded from gray (subpopulation 1) to red (subpopulation 20). Spearman's rank correlation coefficient between yellow and green fluorescence intensities versus C) the temperature of the denaturation midpoint (T_m) of YFP populations, D) the percentage of refolded YFP upon thermal denaturation, and E) the soluble fraction of YFP (in µg/ml) as assessed by an enzyme-linked immunosorbent assay (ELISA). All correlation coefficients are Spearman's rank correlations.

299   To further validate the hypothesis that changes in foldability determine

300   evolutionary changes in trait correlations, we turned to our 20 subpopulations and

301   quantified the overall refolding yield of YFP upon thermal denaturation for these

302   subpopulations. We also measured the temperature of midpoint denaturation (T_m) as a

303   measure of thermodynamic stability, another measure that correlates well with protein

304   foldability[32]. Both measures of protein foldability systematically increased from the first

305   to the 20th subpopulation (Figures 4A-B; Figure S2). Both measures were also

306   themselves highly associated with trait correlations (Figures 4C-E; Spearman's R=0.93

307   and 0.99 for Tm and refolding yield after thermal denaturation, respectively; *p* $\sim 10^{-6}$). In

308   addition, we also used an enzyme-linked immunosorbent assay (ELISA) to measure the

309   amount of soluble protein in each subpopulation, which is also a proxy for protein

310   foldability. Indeed, more soluble YFP subpopulations also fluoresced more intensely

311   (Figure S2). But more importantly, protein solubility was again strongly associated with

312   the magnitude of our trait correlations (R=0.99, *p*$\sim 10^{-6;}$ Spearman's rank correlation).

313   Altogether, these results show that protein foldability is a key determinant of the

314   correlation between the two traits we study.

315   Taken together, our experiments demonstrate that two traits of a single protein

316   can change dramatically and rapidly on short evolutionary time scales through both

317   mutation and selection. What is more, mutations that alter the stability, foldability, and

318   solubility of proteins can cause this change by affecting the fraction of folded, soluble,

319   and fluorescent proteins in each cell.

320   A fluorescent protein fluoresces only in its folded state, but like most other

321   proteins, it can exist in a folded, misfolded, or an unfolded state [32-34]. Any one *E. coli*

322 cell in our experiments contains an ensemble of fluorescent proteins, and within this

323 ensemble, any one protein can randomly transition between these different states. At

324 any instance, each cell thus harbors a fraction of unfolded or misfolded proteins that do

325 not fluoresce. Because these proteins emit neither yellow nor green light, their amount

326 lowers the strength of the correlation between our traits. Indeed, we observed that the

327 fraction of fluorescent cells in our isogenic populations of YFPs not only varied

328 substantially, but was also significantly higher for YFP variants with strong than with

329 weak trait correlations (R=0.87, $p\sim10^{-6;}$ Spearman's rank correlation; Figure S3). In

330 other words, the more foldable a protein is, the longer it remains in the folded state, and

331 the less likely it is to transit to a misfolded or unfolded states. An ensemble of highly

332 foldable proteins can emit green and yellow fluorescence with fewer fluctuations than an

333 ensemble of less foldable proteins, which leads to a stronger correlation between the

334 traits we study.

335 If generally true, our observation that single point mutations can readily change a

336 protein's trait correlations also has implications for correlations between complex traits

337 of higher organisms, and their ability to change over longer evolutionary time scales.

338 Such traits are affected by multiple proteins, and if single mutations can alter trait

339 correlations mediated by at least some of these proteins, these correlations may also be

340 highly malleable in evolution. A recent study that compared correlations between

341 morphological traits of the budding yeast *Saccharomyces cerevisiae* supports the

342 malleability of xomplex traits. It compared correlations in morphological traits observed

343 in single-gene deletion lines of yeast with correlations between the same traits observed

344 in 16 different yeast strains[35]. Many trait pairs showed significantly different correlations

17

345 in the deletion mutants than in the yeast strains, which shows that the correlations

346 between complex traits that involve multiple genes can readily change on the time

347 scales on which new yeast strains evolve.

348   The main biophysical property that make trait correlations malleable in our

349 experiments is foldability. This property is essential for the function of most proteins[36-39].

350 It can also readily change by mutations. Specifically, most random mutations in proteins

351 are destabilizing[40], but ~20% of such mutations are stabilizing and increase protein

352 foldability[40]. In consequence, protein foldability is highly variable during protein

353 evolution[41-44]. For example, even though the ability to bind oxygen does not differ

354 substantially among mammalian myoglobins (oxygenation constant ~ 0.8-1.2 μM^{-1}), the

355 unfolding transitions of these myoglobins differ nearly 600-fold in their resistance to

356 chemical denaturants[44,45]. Other well-studied proteins include the essential bacterial

357 dihydrofolate reductase (DHFR), which reduces dihydrofolic acid to tetrahydrofolic

358 during folate biosynthesis, as well as mammalian superoxide dismutase 1 (SOD1),

359 which reduces superoxides to hydrogen peroxides to destroy damaging free superoxide

360 radicals. Mutations that affect the stability of these proteins' secondary and tertiary

361 structures also alter their foldability [46-48]. More generally, proteins in the proteomes of *E.*

362 *coli*, *C. elegans*, *S. cerevisiae*, and human vary widely in their thermodynamic

363 stability[49,50], which correlates with protein foldability[32]. These examples show that

364 changes in protein foldability are frequent in the evolution of proteins. As our work

365 showed, such changes can also lead to substantial changes in trait correlations. Such

366 malleable trait correlations caused by changes in protein foldability can facilitate the co-

367 evolution or individuation of simple or complex traits in evolution.

368   In sum, our experiments not only show that correlations between traits of a single

369   protein can change rapidly and on short evolutionary time scales. They also provide a

370   simple biophysical explanation for this change. They link the fundamental protein

371   property of foldability with a fundamental aspect of evolvability – trait correlations. In

372   doing so, they can help explain how evolvability can evolve rapidly.

373

382
383
384
385
386
387
388
389
390
391
392
393
394
395   **Materials and Methods:**

Plasmids, strains, and mutant libraries

We used the vector pBAD202/D-TOPO (K4202-01, Invitrogen), which carries an arabinose-inducible araBAD promoter and a Kanamycin-resistance gene for YFP evolution within the E. coli strain BW27783 (CGSC 12119). As described previously[3], we inserted the coding region of *yfp* from water jellyfish (*Aequorea victoria;* Uniprot ID: A0A059PIR9) that was already present in the plasmid pAND[2] into the vector backbone of pBAD202/D-TOPO by restriction digest and ligation. We inserted the YFP-coding gene between *Xho*I and *Hind*III restriction sites, placing it under the control of the arabinose-inducible *araBAD* promoter. We named the resulting plasmid pBAD-YFP.

We introduced random mutations into the coding region of YFP by mutagenic PCR as previously described[3]. Briefly, we added 10 ng of template plasmid to 100 µl of a PCR reaction mix that contains 10 µl of 10×ThermoPol buffer (M0267L, NEB), 2.5 µl of *Taq* DNA polymerase (M0267L, NEB), 400 µM of dNTPs (R0192, Thermo Scientific), 3 µM of 8-oxo-GTP/dPTP (Trilink Biotechnologies), and 400 nM of each primer (MutafpF- GAAGGAGATATACctcgag /MutafpR- AGACCGTTTAAACaagctt). We used a Biometra thermocycler to perform PCR by using the following program: 95 °C/30 s; 25 cycles of 94 °C/20 s, 46 °C/30 s and 68 °C/50 s; 68 °C/5 min. We used the restriction enzymes *Xho*I and *Hind*III (R0146L/R3104S, NEB) to digest the resulting PCR products, and used *Dpn*I (R0176S, NEB) to remove the template plasmid by following the manufacturer's protocols. We used the QIAquick PCR purification kit to purify the digested mutated YFP pools to obtain linearized inserts.

Sorting cells from a pool of evolving populations at the end of directed evolution

To systematically study how selection affects protein evolvability through direct effects on fitness and indirect effects on protein stability and foldability, we sampled diverse YFP variants that vary broadly in yellow fluorescence. Specifically, we sampled from YFP populations in a previously published directed evolution experiment, in which we had evolved populations of YFP under either strong selection for yellow fluorescence (populations S, top 20 percent of yellow fluorescing cells survive selection), weak selection (populations W, top 65 percent survive), or no selection (populations N for neutral, 100 percent survive)[30]. For each of these selection regimes we had evolved four replicate populations for four rounds ("generations") of directed evolution through fluorescent activated cell sorting (FACS)-based selection and PCR-based mutagenesis.

To create a pool of yellow fluorescent proteins that cover a broad range of fluorescence intensities, we sampled 100 µl of glycerol stock from each of the four replicate S populations (from generation 4), W populations (generation 4), and W populations (generation 2). We added to each of these 12 (=4+4+4) samples 2 ml LB medium supplemented with 30 µg/ml kanamycin. We grew the resulting 12 cultures at 37 °C with shaking at 220 rpm in a 10 ml tube for ~5 h, and then transferred 50 µl of each culture to 2 ml LB supplemented with 30 µg/ml kanamycin. After continuing cultivation for another ~12 h, we combined 400 µl of each culture into one tube and mixed thoroughly. Subsequently, we added 900 µl of the resulting mixture into 600 µl 50% glycerol and stored it at -80 °C for the subsequent sorting experiments. We call the

21

438   resulting mixture our "pooled" population of YFP-expressing cells. We sorted this pooled

439   populations into 20 "subpopulations" as shown in Figure 2A.

440   To sort the pooled population into 20 subpopulations according to their

441   fluorescence, we first added 200 μl of glycerol stock of the pooled population sample to

442   3 ml LB medium containing 30 μg/ml kanamycin, and grew the resulting culture at 37 °C

443   with shaking at 220 rpm for ~5 h. We then transferred 200 μl of the culture into 20 ml LB

444   medium with 50 μg/ml kanamycin, and continued the incubation for ~12 h. We then

445   sampled 2 ml of the culture and centrifuged it at 9,000 g and 4 °C for 5 min to collect

446   cells. We suspended the collected cells in 2 ml LB medium supplemented with 50 μg/ml

447   of kanamycin and 0.2% arabinose, and continued cultivation for ~12 h. Subsequently,

448   we sampled 40 μl of culture and suspended it in 2 ml cold PBS buffer. We selected cells

449   by their yellow fluorescence intensity according to the selection criteria described in

450   Figures 2A-B with an Aria III cell sorter (BD Biosciences). Specifically, we sorted cells at

451   4 °C in the FITC channel (λex = 488 nm, λem = 530±15 nm), and collected 10^5 cells in

452   ~1 ml LB medium for each sorted subpopulation. We placed the selected cells on ice

453   until we had finished sorting all subpopulations to prevent cell proliferation or death. We

454   prepared a glycerol stock of each subpopulation for later flow cytometry measurements.

455   **Fluorescence assay using flow cytometry**

456   We added 200 μl of glycerol stock from each subpopulation into 10 ml LB medium

457   containing 50 μg/ml of kanamycin, and incubated the resulting 20 cultures at 37 °C with

458   shaking at 220 rpm for ~8 h. We then sampled 2 ml of each subpopulation's culture, and

459   centrifuged it at 9000 g and 4°C to collect cells. To the pelleted cells of each

460   subpopulation we added 2.3 ml LB medium supplemented with 50 µg/ml of kanamycin

461   and 0.2% arabinose, resuspended the cells, and grew the resulting culture at 37 °C with

462   shaking at 220 rpm for ~12 h. This procedure yielded 20 overnight cultures. We then

463   added 20 µl of these 20 overnight cultures to 180 µl of cold PBS buffer. After mixing

464   thoroughly by pipetting, we transferred 5 µl of the resulting suspension into 195 µl of

465   cold PBS buffer, mixed thoroughly, and measured yellow fluorescence in the FITC

466   channel ($λ_{ex}$ = 488 nm and $λ_{em}$ = 530 ± 15 nm) and green fluorescence in the AmCyan

467   channel ($λ_{ex}$ = 405 nm and $λ_{em}$ = 525 ± 25 nm) at room temperature. We used a

468   Fortessa cell analyzer (BD Biosciences) to analyze ~10^4 events per biological replicate

469   with a flow rate of ~3000 events/s. We sorted three biological replicates for each

470   subpopulation We placed all samples on ice during sample analysis to prevent cell

471   proliferation or death.

472   **Flow cytometry data analysis**

473   We used FlowJo V10.4.2 (LLC) to analyze flow cytometry data. Specifically, we first

474   selected a homogenous cell population by forward scatter height (FSC-H) versus side

475   scatter height (SSC-H) density plots. We then selected singlets (single cells) by using

476   side scatter area (SSC-A) versus side scatter height (SSC-H) density plots. We used

477   the resulting filtered data for determining green and yellow fluorescence intensities.

478   **Extracting soluble fluorescent proteins**

479   After inducing the expression of YFP variants in each subpopulation as described in

480   *Fluorescence assay using flow cytometry*, we sampled 2 ml of the overnight culture of

23

481   each subpopulation for extracting soluble fluorescent proteins by following the

482   manufacturer's protocol. Specifically, we centrifuged the culture for each subpopulation

483   at 5,000g and at 4 °C for 5 min to collect cells, and stored the collected cells at -20 °C

484   overnight. We then followed the manufacturer's protocol to extract soluble proteins by

485   using CelLytic™ B Cell Lysis Reagent (B7435-500ml, Sigma). Subsequently, we used

486   200 µl cell lysis solution (ThermoFisher; 50 mM Tri with pH 7.4, 250 mM NaCl, 5mM, 50

487   mM NaF, 1mM Na_3VO_4, 0.02% NaN3) to dissolve the soluble proteins, and placed the

488   resulting soluble pellet sample on ice for subsequent experiments.

489   **Protein refolding assay**

490   To unfold fluorescent proteins, we mixed 5 µl of crude lysate of each subpopulation with

491   45 µl of 8M urea (containing 10 mM DTT), and heated the sample at 95 °C for 5 min in a

492   PCR thermocycler. Asa control, we mixed 5 µl of crude lysate with 45 µl of TNG buffer

493   (100 mM Tris, 100 mM NaCl, 10% glycerol, 10 mM DTT, 1×cOmplete™ (EDTA-free

494   Protease Inhibitor Cocktail, Roche 11873580001), pH 7.2-7.5). To refold the unfolded

495   fluorescent proteins, we rapidly added 10 µl aliquots of an unfolded sample or of the

496   control into 190 µl of TNG buffer in a 96 well microplate, and immediately measured

497   fluorescence intensity using an infinite F200 Pro microplate reader (λex = 485 nm, λem

498   = 530 nm). We measured fluorescence at ~20 min intervals with 2-mm orbital shaking in

499   between. We report the refolding yields as fluorescence relative to the control.

Protein thermal stability assay

500

501   To quantify the thermal stability of fluorescent proteins in each subpopulation, we added

502   2 µl of crude lysate to 98 µl of TNG buffer, and mixed thoroughly by pipetting. We

503   incubated the resulting mixture in a PCR cycler for 5 min, and subjected each

504   subpopulation to a temperature range of 60.6-80.6 °C (specifically, 60.6, 62, 64.1, 66.6,

505   69, 71.6, 74, 76.5, 78.6, 80 and 80.6 °C), followed by a 30 second incubation at 4 °C.

506   Then we immediately transferred 90 µl of each mixture to a 96 well microplate, and

507   used an infinite F200 Pro (λex = 485 nm, λem = 530 nm) to measure its fluorescence

508   intensity. As a control, we used the unheated lysate-buffer mixture. We report thermal

509   stability as fluorescence relative to the control.

Quantification of soluble fluorescent proteins by ELISA

510

511   To quantify the amount of soluble fluorescent proteins in each subpopulation, we used a

512   GFP ELISA Kit (AKR-121, Cell Biolabs Inc.) which can detect GFP, BFP, CFP, and YFP

513   from *Aequorea victoria*. Specifically, we followed the manufacture's protocol to

514   determine the quantity of soluble fluorescent proteins in the lysate of each biological

515   replicate for every subpopulation by comparing its absorbance with that of a

516   recombinant GFP standard curve.

Fluorescence assay using a microplate reader

517

518   To further validate how different selection strengths affect the association between

519   green and yellow fluorescence, we randomly sampled 90 clones from each of the

25

520   twenty subpopulations, and measured their green and yellow fluorescence intensities

521   using a microplate reader. Specifically, we used saline to dilute the glycerol stock of

522   each subpopulation 10^5-fold, and plated 100 µl of the resulting culture on LB agar

523   supplemented with 25 µg/ml kanamycin. We incubated the LB agar plates in an

524   incubator at 37 °C overnight, picked single colonies, and inoculated each colony into

525   200 µl of LB medium (50 µg/ml kanamycin). We grew the resulting cultures in a

526   microplate incubator at 37 °C and 1000 rpm. After ~5 h of incubation, we transferred 50

527   µl of each culture into 150 µl LB medium supplemented with 0.2% (w/v) arabinose and

528   50 µg/ml kanamycin, and continued the incubation for ~16 h. We then mixed 50 µl of

529   each culture with 170 µl PBS buffer by pipetting thoroughly, and used a TECAN

530   microplate reader (TECAN Spark) to measure both yellow (λex = 485 nm, λem = 530

531   nm) and green (λex = 400 nm, λem = 512 nm) fluorescence intensities.

532

533   **Statistical analyses**

534   To test the null hypothesis that trait correlations are identical between samples (e.g.,

535   when comparing trait correlations between two subpopulations), we used Fisher's z-

536   transformation. In this approach, Pearson's or Spearman's correlation coefficients are

537   converted to z-scores, so that they become normally distributed. The null hypothesis is

538   then tested using a t-test on the z-scores. We performed all statistical analyses with R

539   (v.4.0)[51].

540
541
542   **References**
543

544   1.   Payne, J.L. & Wagner, A. The causes of evolvability and their evolution. *Nature Reviews Genetics* **20**, 24-38 (2019).
545   2.   Wintrode, P.L. & Arnold, F.H. Temperature adaptation of enzymes: lessons from laboratory evolution. *Advances in*
546   *protein chemistry* **55**, 161-225 (2001).

547 3.   Saltz, J.B., Hessel, F.C. & Kelly, M.W. Trait correlations in the genomics era. *Trends in ecology & evolution* **32**, 279-290
548   (2017).
549 4.   Svensson, E.I. *et al.* Correlational selection in the age of genomics. *Nature ecology & evolution* **5**, 562-573 (2021).
550 5.   Sgrò, C.M. & Hoffmann, A.A. Genetic correlations, tradeoffs and environmental variation. *Heredity* **93**, 241-248
551   (2004).
552 6.   Group, D.P.C. Weight-height relationships and body mass index: some observations from the Diverse Populations
553   Collaboration. *American journal of physical anthropology* **128**, 220-229 (2005).
554 7.   Colosimo, P.F. *et al.* Widespread parallel evolution in sticklebacks by repeated fixation of ectodysplasin alleles. *science*
555   **307**, 1928-1933 (2005).
556 8.   Thomas, J.W. *et al.* The chromosomal polymorphism linked to variation in social behavior in the white-throated
557   sparrow (Zonotrichia albicollis) is a complex rearrangement and suppressor of recombination. *Genetics* **179**, 1455-
558   1468 (2008).
559 9.   Huo, H., Wei, S. & Bradford, K.J. DELAY OF GERMINATION1 (DOG1) regulates both seed dormancy and flowering time
560   through microRNA pathways. *Proceedings of the National Academy of Sciences* **113**, E2199-E2206 (2016).
561 10.   Wagner, G.P., Pavlicev, M. & Cheverud, J.M. The road to modularity. *Nature Reviews Genetics* **8**, 921-931 (2007).
562 11.   Lande, R. The genetic correlation between characters maintained by selection, linkage and inbreeding. *Genetics*
563   *Research* **44**, 309-320 (1984).
564 12.   Lande, R. The genetic covariance between characters maintained by pleiotropic mutations. *Genetics* **94**, 203-215
565   (1980).
566 13.   Lande, R. Quantitative genetic analysis of multivariate evolution, applied to brain: body size allometry. *Evolution*, 402-
567   416 (1979).
568 14.   Wagner, G.P. & Altenberg, L. Perspective: complex adaptations and the evolution of evolvability. *Evolution* **50**, 967-
569   976 (1996).
570 15.   Revell, L.J. Size-correction and principal components for interspecific comparative studies. *Evolution: International*
571   *Journal of Organic Evolution* **63**, 3258-3268 (2009).
572 16.   Collar, D.C., Near, T.J. & Wainwright, P.C. Comparative analysis of morphological diversity: does disparity accumulate
573   at the same rate in two lineages of centrarchid fishes? *Evolution* **59**, 1783-1794 (2005).
574 17.   Young, N.M. & Hallgrĺmsson, B. Serial homology and the evolution of mammalian limb covariation structure. *Evolution*
575   **59**, 2691-2704 (2005).
576 18.   Dececchi, T.A. & Larsson, H.C. Body and limb size dissociation at the origin of birds: uncoupling allometric constraints
577   across a macroevolutionary transition. *Evolution* **67**, 2741-2752 (2013).
578 19.   Arendt, D. *et al.* The origin and evolution of cell types. *Nature Reviews Genetics* **17**, 744-757 (2016).
579 20.   Blein, T., Hasson, A. & Laufs, P. Leaf development: what it needs to be complex. *Current opinion in plant biology* **13**,
580   75-82 (2010).
581 21.   Wagner, G.P. & Lynch, V.J. Evolutionary novelties. *Current Biology* **20**, R48-R52 (2010).
582 22.   Navalón, G., Marugán-Lobón, J., Bright, J.A., Cooney, C.R. & Rayfield, E.J. The consequences of craniofacial integration
583   for the adaptive radiations of Darwin's finches and Hawaiian honeycreepers. *Nature Ecology & Evolution* **4**, 270-278
584   (2020).
585 23.   Wright, I. *et al.* A survey of seed and seedling characters in 1744 Australian dicotyledon species: cross-species trait
586   correlations and correlated trait-shifts within evolutionary lineages. *Biological Journal of the Linnean Society* **69**, 521-
587   547 (2000).
588 24.   Guillaume, F. & Chebib, J. Pleiotropy or linkage? Their relative contributions to the genetic correlation of quantitative
589   traits and detection by multitrait GWA studies. *Genetics* **219**, iyab159 (2021).
590 25.   Van Voorhies, W.A. Bergmann size clines: a simple explanation for their occurrence in ectotherms. *Evolution* **50**, 1259-
591   1264 (1996).
592 26.   Gutteling, E. *et al.* Environmental influence on the genetic correlations between life-history traits in Caenorhabditis
593   elegans. *Heredity* **98**, 206-213 (2007).
594 27.   Andersson, H., Baechi, T., Hoechl, M. & Richter, C. Autofluorescence of living cells. *Journal of microscopy* **191**, 1-7
595   (1998).
596 28.   Raser, J.M. & O'shea, E.K. Noise in gene expression: origins, consequences, and control. *Science* **309**, 2010-2013
597   (2005).
598 29.   Kaufmann, B.B. & van Oudenaarden, A. Stochastic gene expression: from single molecules to the proteome. *Current*
599   *opinion in genetics & development* **17**, 107-112 (2007).
600 30.   Zheng, J., Guo, N. & Wagner, A. Selection enhances protein evolvability by increasing mutational robustness and
601   foldability. *Science* **370**(2020).
602 31.   Zheng, J., Payne, J.L. & Wagner, A. Cryptic genetic variation accelerates evolution by opening access to diverse
603   adaptive peaks. *Science* **365**, 347-353 (2019).

32.   Reddy, G., Liu, Z. & Thirumalai, D. Denaturant-dependent folding of GFP. *Proceedings of the National Academy of Sciences* **109**, 17832-17838 (2012).

33.   Huang, J.-r., Craggs, T.D., Christodoulou, J. & Jackson, S.E. Stable intermediate states and high energy barriers in the unfolding of GFP. *Journal of molecular biology* **370**, 356-371 (2007).

34.   Dietz, H. & Rief, M. Exploring the energy landscape of GFP by single-molecule mechanical experiments. *Proceedings of the National Academy of Sciences* **101**, 16192-16197 (2004).

35.   Jiang, D. & Zhang, J. Detecting natural selection in trait-trait coevolution. *bioRxiv* (2021).

36.   Govindarajan, S. & Goldstein, R.A. Evolution of model proteins on a foldability landscape. *Proteins: Structure, Function, and Bioinformatics* **29**, 461-466 (1997).

37.   Govindarajan, S. & Goldstein, R.A. The foldability landscape of model proteins. *Biopolymers: Original Research on Biomolecules* **42**, 427-438 (1997).

38.   Shakhnovich, E. Protein folding thermodynamics and dynamics: where physics, chemistry, and biology meet. *Chemical reviews* **106**, 1559-1588 (2006).

39.   Shakhnovich, E.I. Theoretical studies of protein-folding thermodynamics and kinetics. *Current opinion in structural biology* **7**, 29-40 (1997).

40.   Tokuriki, N., Stricher, F., Schymkowitz, J., Serrano, L. & Tawfik, D.S. The stability effects of protein mutations appear to be universally distributed. *Journal of molecular biology* **369**, 1318-1332 (2007).

41.   Dasmeh, P. & Serohijos, A.W.R. Estimating the contribution of folding stability to nonspecific epistasis in protein evolution. *Proteins* **86**, 1242-1250 (2018).

42.   Dasmeh, P. & Serohijos, A.W. Estimating the contribution of folding stability to nonspecific epistasis in protein evolution. *Proteins: Structure, Function, and Bioinformatics* **86**, 1242-1250 (2018).

43.   Dasmeh, P., Girard, É. & Serohijos, A.W. Highly expressed genes evolve under strong epistasis from a proteome-wide scan in E. coli. *Scientific reports* **7**, 15844 (2017).

44.   Dasmeh, P., Serohijos, A.W., Kepp, K.P. & Shakhnovich, E.I. Positively selected sites in cetacean myoglobins contribute to protein stability. *PLoS computational biology* **9**, e1002929 (2013).

45.   Scott, E.E., Paster, E.V. & Olson, J.S. The stabilities of mammalian apomyoglobins vary over a 600-fold range and can be enhanced by comparative mutagenesis. *Journal of Biological Chemistry* **275**, 27129-27136 (2000).

46.   Razban, R.M., Dasmeh, P., Serohijos, A.W. & Shakhnovich, E.I. Avoidance of protein unfolding constrains protein stability in long-term evolution. *Biophysical Journal* (2021).

47.   Dasmeh, P. & Kepp, K.P. Superoxide dismutase 1 is positively selected to minimize protein aggregation in great apes. *Cellular and Molecular Life Sciences*, 1-15 (2017).

48.   Bershtein, S. *et al.* Protein homeostasis imposes a barrier on functional integration of horizontally transferred genes in bacteria. *PLoS genetics* **11**, e1005612 (2015).

49.   Ghosh, K. & Dill, K. Cellular proteomes have broad distributions of protein stability. *Biophysical journal* **99**, 3996-4002 (2010).

50.   Leuenberger, P. *et al.* Cell-wide analysis of protein thermal unfolding reveals determinants of thermostability. *Science* **355**(2017).

51.   Team, R.C. R: A language and environment for statistical computing. (2013).